Martin et al. Supplemental Material

Supplemental Video. Focal adhesions are less dynamic in Nck1/Nck2 double knockout podocytes.

Supplementa1 Table 1: Antibody information for immunoprecipitation experiments.

Supplemental Table 2: Antibody information for immunoblotting experiments.

Supplemental Table 3: Antibody information for immunofluorescent experiments.

Supplemental Table 4: Sequences used for CRISPR-Cas9 gene editing and TIDE analysis.

Supplemental Table 5: Primers used for semi-quantitative real-time reverse transcriptase polymerase chain reaction.

Supplemental Table 6: Primers used for genotyping.

Supplemental Figure 1. Generation of wildtype and Nck1 and Nck2 double knockout mouse podocyte cell lines.

Supplemental Figure 2. Gene expression analysis of wildtype and Nck1 and Nck2 double knockout podocytes.

Supplemental Figure 3. Normalized enrichment scores from gene set enrichment analysis of microarray data.

Supplemental Figure 4. Multi-faceted contributions of Nck1 and Nck2 to α actinin-4 and ß1 integrin-related cell adhesion.

Supplemental Figure 5. Loss of Nck1 or Nck2 (but not Nck1/2 haploinsufficiency) results in biochemical abnormalities and susceptibility to disease.

Supplemental References

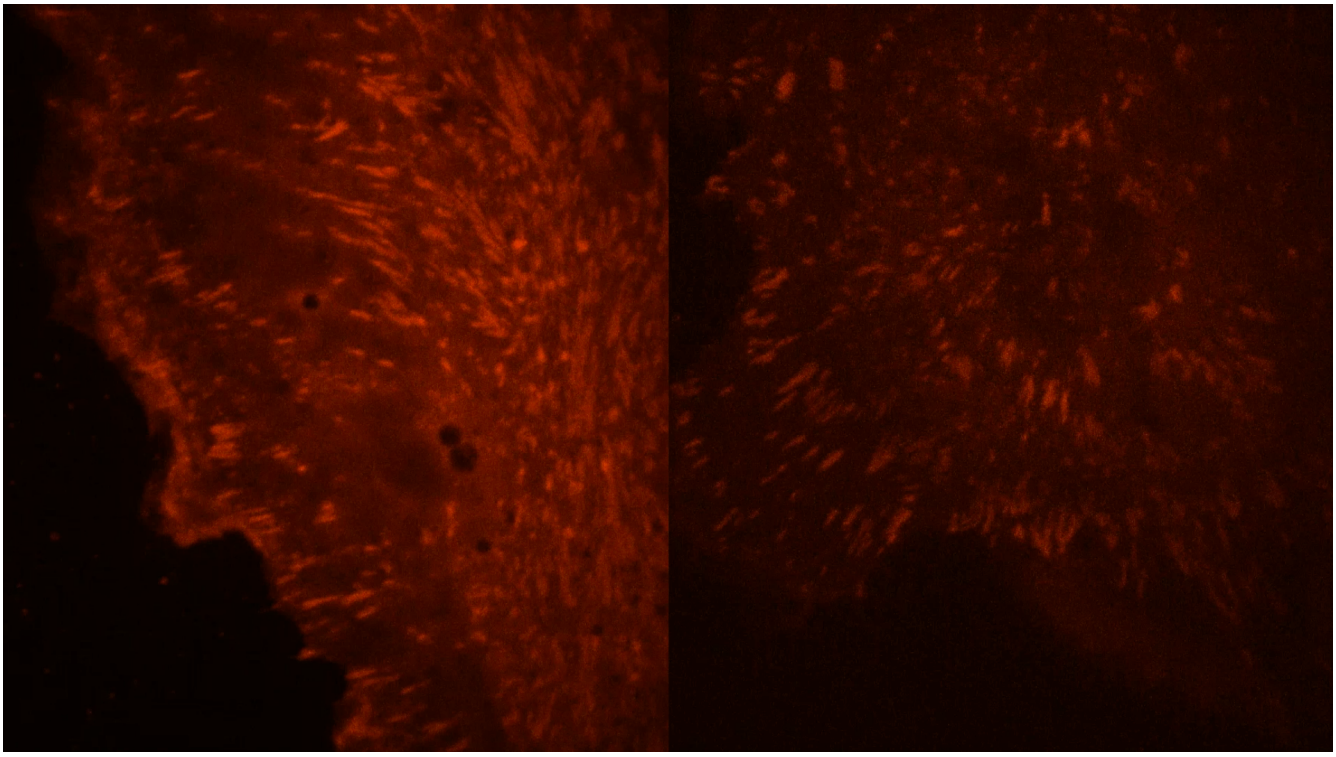

Supplemental Video. Focal adhesions are less dynamic in Nck1/Nck2 double knockout podocytes. Wildtype (left) and Nck1/2 double knockout (right) podocytes were transduced with paxillin-mCherry adenovirus. Images were taken each minute for 22 minutes to profile focal adhesion dynamics. 100x optical zoom. Video file available online in Supplemental Material section.

Supplemental Table 1: Antibody information for immunoprecipitation experiments. Pr-A: proteinA-sepharose beads.

Immunoprecipitation			
Antibody	Species	Source	Concentration
anti–IgG	rabbit	Cell signalling; 2729	1ul/ 100ul Pr-A beads
anti–Nck (1794)	rabbit	Larose Lab[83]	1ul/ 100ul Pr-A beads
anti–α actinin 4	rabbit	Abcam; ab108198	1ul/ 100ul Pr-A beads
Magnetic anti–FLAG beads	mouse	Sigma; M8823	20 μL of a 50% magnetic anti-FLAG M2 beads/ IP

Supplemental Table 2: Antibody information for immunoblotting experiments.

Western Immunoblotting			
Antibody	Species	Source	Concentration
anti–GAPDH	mouse	Applied Biologic Materials Inc.; G041	1:1000
anti–*β*-actin	mouse	Sigma-Aldrich; A5441	1:2000
anti–Nck (1794)	rabbit	Larose Lab[83]	1:1000
anti–mouse HRP	goat	Bio-Rad; 170–6516	1:10000
anti–rabbit HRP	goat	Bio-Rad; 170–6515	1:10000
anti–FLAG M2	mouse	Sigma-Aldrich; F3165	1:2000
anti–WT-1 (C-19)	rabbit	Santa Cruz; sc-192	1:500
anti–eplin	rabbit	Thermo Proteintech; 16639-1-AP	1:2000
anti–palladin	rabbit	Thermo Proteintech; 10853-1-AP	1:2000
anti–p130-Cas	mouse	BD Biosciences; 610272	1:1000
anti–Fak	rabbit	Millipore; 04-591	1:1000
anti–actin	rabbit	Cytoskeleton; AAN01	1:500
anti– *β*1 integrin	mouse	Santa Cruz; sc-9970	1:1000
anti–Nck	mouse	BD Biosciences; N15920	1:1000
anti– α actinin-4	rabbit	Abcam; ab108198	1:2000

Supplemental Table 3: Antibody information for immunofluorescent experiments.

Immunofluorescence			
Antibody	Species	Source	Concentration
anti–nephrin	guinea pig	20R-NP002; Fitzgerald Inc.	1:100
anti–synaptopodin	mouse	Fitzgerald; 10R-2373	1:150
anti–WT-1	rabbit	Santa Cruz; sc-192)	1:50
anti–paxillin	rabbit	Santa Cruz; sc-5574	1:50
anti–paxillin	rabbit	Abcam; Ab32054	1:100
anti–paxillin 5H-11	mouse	Upstate; 05-417	1:100
anti–β1 integrin	rat	Millipore; MAB1997	1:500
anti–active β1 integrin	rat	BD Biosciences; BD550531	1:50
anti–laminin a5	mouse	DSHB P3H9	neat
TexasRed phalloidin	-	T7471; Invitrogen	1:50
Phalloidin-647	-	A30107; Invitrogen	1:100
anti–Alpha actinin-4	rabbit	Abcam; ab108198	1:100
anti–FLAG-M2	mouse	Sigma; F3165	1:100
anti–rabbit Alexa Fluor 488	goat	A11008; Invitrogen	1:400
anti–rabbit Alexa Fluor 594	goat	A11076; Invitrogen	1:400
anti–mouse Alexa Fluor 488	goat	A11001; Invitrogen	1:400
anti–mouse Alexa Fluor 594	goat	A11005; Invitrogen	1:400
anti–rat Alexa Fluor 488	goat	A11006; Invitrogen	1:400
anti–guinea pig Alexa Fluor 594	goat	A11076; Invitrogen	1:400

Supplemental Table 4: Sequences used for CRISPR-Cas9 gene editing and TIDE analysis. FW, forward; RV, reverse.

Gene Target	Guide Sequence (FW/RV)	TIDE Primer (FW/RV)	TIDE Efficiency
Actn4	TACCAGTACGGCCCGAACAG	AGTTCCATTGCAACCTCCCG	93.9%
	CTGTTCGGGCCGTACTGGTAC	CATTCATGACTTGGGCCCCG	
Palld	ACGGAAGCTTCGCTTCAAGG	TGCCATCAGTACTTCCGTGT	90.9%
	CCTTGAAGCGAAGCTTCCGTC	CCCTATGGGTGTCCGAACCT	
Lima1	TCGTGGCTGTTCTCTGAGCG	n/a	undetermined
	CGCTCAGAGAACAGCCACGAC	n/a	

Supplemental Table 5: Primers used for semi-quantitative real-time reverse transcriptase polymerase chain reaction. FW, forward; RV, reverse.

Gene target	Primer (FW/RV)	Harvard primer bank number
Gapdh	AGGTCGGTGTGAACGGATTT	
	GGGGTCGTTGATGGCAACA	
Hprt	CATGGACTGATTATGGACAGG	
	ATCCAGCAGGTCAGCAAAGAA	
Nck1	GCGGTCCTCAGGTGACTGG	
	ATTCATGGAATTTCGAACTCGCCAC	
Nck2	AGGACAGGCTACGTGCCTT	
	GTACTCCGCATCAGTGCTTGG	
Mmp2	CAAGTTCCCCGGCGATGTC	6678902a1
	TTCTGGTCAAGGTCACCTGTC	
Mmp13	CTTCTTCTTGTTGAGCTGGACTC	6678896a1
	CTGTGGAGGTCACTGTAGACT	
Intav	GGGCCTATTGTTCAGCACAT	
	GATTCCACAGCCCAAAGTGT	
Intb3	GTAATCGAGATGCCCCAGAG	
	CTTCCATCCAGGGCAATATG	
Inta3	TGCCGTTCTAAATCCTCCAC	
	CACCGGTAGTCAGGCAATTT	
Intb1	GGTGTCGTGTTTGTGAATGC	
	TCCTGTGCACACGTGTCTT	
Lama5	ACCCAAGGACCCACCTGTAG	
	TCATGTGTGCGTAGCCTCTC	
Lamb2	CGTGACCATCCAACTGGACCTGG	
	CCAAGCCTTCCCAAAGTCAGAAG	
Col4a1	CTGGCACAAAAGGGACGAG	33859528a1
	ACGTGGCCGAGAATTTCACC	
Col4a2	GACCGAGTGCGGTTCAAAG	556299a1
	CGCAGGGCACATCCAACTT	
Col4a3	CAAAGGCATCAGGGGAATAACT	6680968a1
	ATCCGTTGCATCCTGGTAAAC	
Col4a4	ATGAGGTGCTTTTTCAGATGGAC	34328045a1
	GGGGCCGCCATACTTCTTG	
Col4a5	AGGCGAAATGGGTATGATGGG	26348681a1
	CTCCCTTACCGCCCTTTTCTC	
Col5a2	CCCTGGCTTGAAAGGTCACAG	86613789c3
	GCCCATAGCACCCATTGGAC	
Col1a1	TAAGGGTACCGCTGGAGAAC	
	GTTCACCTCTCTCACCAGCA	
Fn1	ATGTGGACCCCTCCTGATAGT	
	GCCCAGTGATTTCAGCAAAGG	

Supplemental Table 6: Primers used for genotyping. FW, forward; RV, reverse; Podo-dKO, podocyte-specific Nck1/Nck2 double knockout; KO, knockout.

Gene target	Primer (FW/RV)	Mouse line
Cre	GCAGAACCTGAAGATGTTCGC	Podo-dKO
	GCACGTTCACCGGCATCAACG	
Rtta	CGCACTTCAGTTACTTCAGGTCCTC	Podo-dKO
	GCTTATGCCTGATGTTGATGATGC	
Nck1 WT	GCATGTAGACAATTACACTTCAGCACC	Podo-dKO Nck1KO
	ATTCATGGAATTTCGAACTCGCCACC	
Nck1 lacZ	CTGATTGAAGCAGAAGCCTGCGATG	Podo-dKO Nck1KO
	TATTGGCTTCATCCACCACATACAGG	
Nck2 flox	GGATACCACATTGGCATTAGTAG	Podo-dKO
	GTGCTCATTTGACAAGTGACAC	
Nck2KO WT	CTACACTGCCCAGCAGGACCAGG	Nck2KO
	CACATACAGATACACACACGCTGAAG	
Nck2KO KO	CCAATGGCAAAGGTGATCATGACGG	Nck2KO
	CGCCTTCTATCGCCTTCTTGACGAG	

Supplementary figure 1

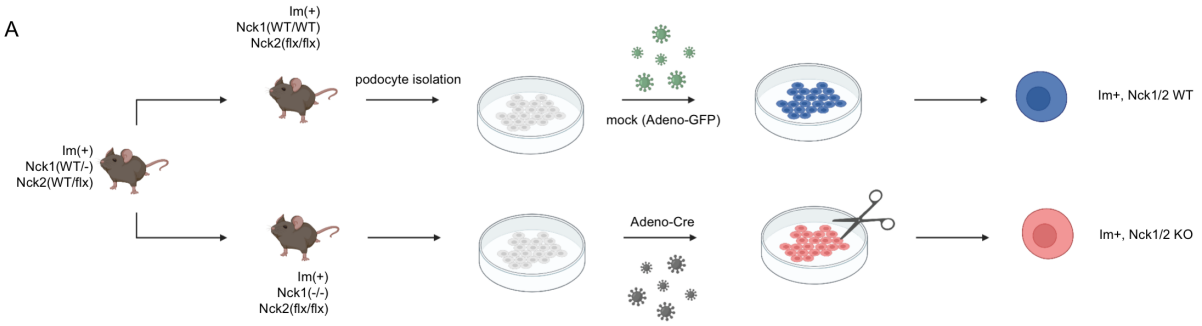

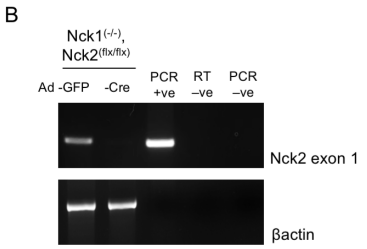

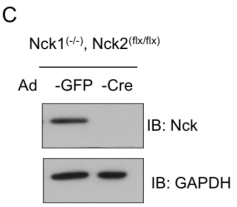

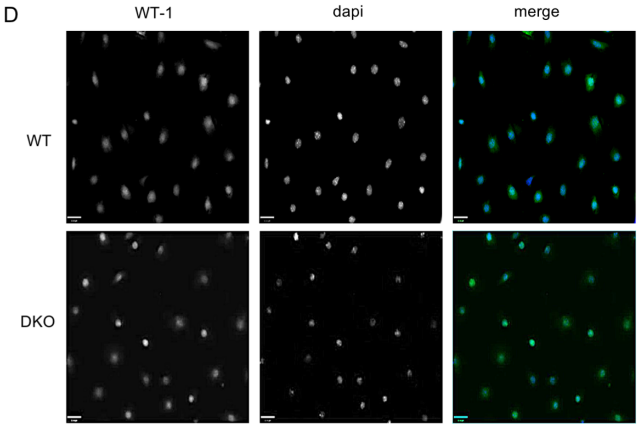

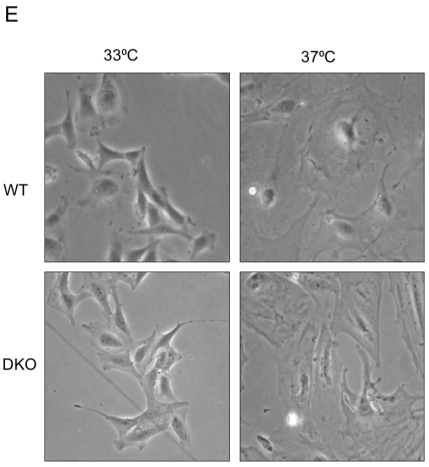

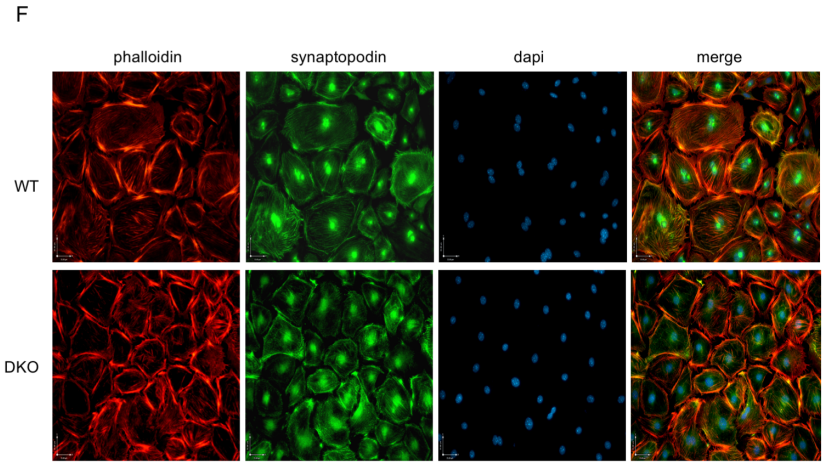

Supplemental Figure 1. Generation of wildtype and Nck1 and Nck2 double knockout mouse podocyte cell lines. (A) Scheme for generation of wildtype (WT) and Nck1 and Nck2 double knockout (dKO) conditionally immortalized mouse podocyte cell lines (MPCs). (B) Reverse transcriptase polymerase chain reaction (RT PCR) demonstrating adenoviral expression of Cre (adeno-Cre) but not mock (adeno-GFP) allows for targeted excision of floxed Nck2 and the generation of dKO cells. (C) Western immunoblot (IB) validating knockout of Nck1 and Nck2 in podocyte cell lines. (D) Immunofluorescent (IF) imaging of Wilm's Tumour (WT)-1 in WT and dKO podocytes. (E) Phase-contrast images of WT and dKO MPCs cultured under permissive (33ºC, IFNγ supplementation) and differentiating (37ºC) conditions. (F) IF imaging of phalloidin and synaptopodin in WT and dKO MPCs.

Supplementary figure 2

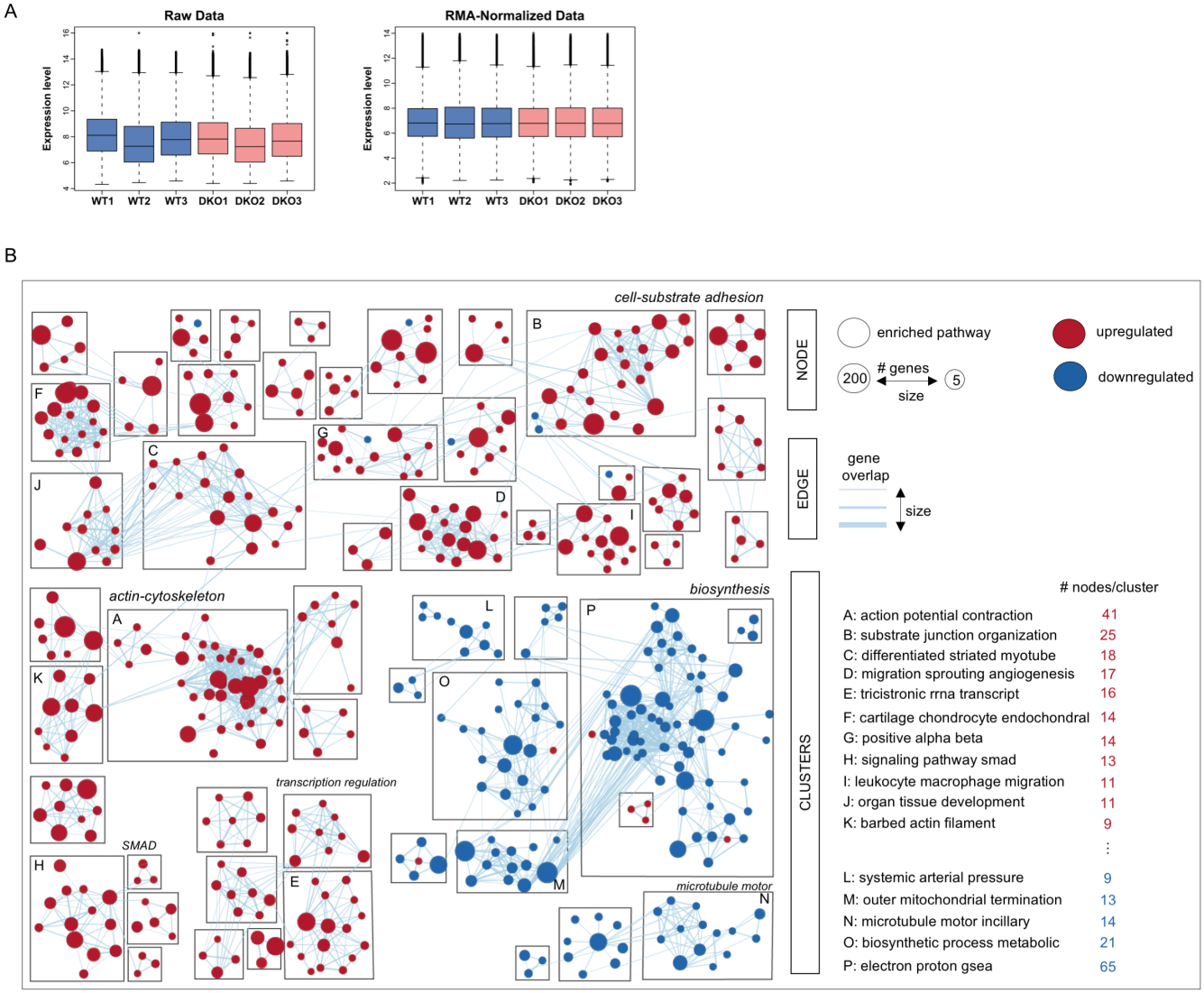

Supplemental Figure 2. Gene expression analysis of wildtype and Nck1 and Nck2 double knockout podocytes. (A) BoxPlots of raw and RMA-normalized microarray data from 3 biological replicates. (B) Gene set enrichment analysis (GSEA) map generated from microarray of WT and dKO MPCs (FDR *Q* value < 0.05 and combined coefficient >0.375 with combined constant = 0.5). Red and blue nodes represent up- and down-regulated genes respectively. Node size is proportional to the number of genes per term. Node clusters were labelled using AutoAnnotate following manual organization in Cytoscape. Labels for minimally interconnected networks were removed for clarity.

Supplementary figure 3

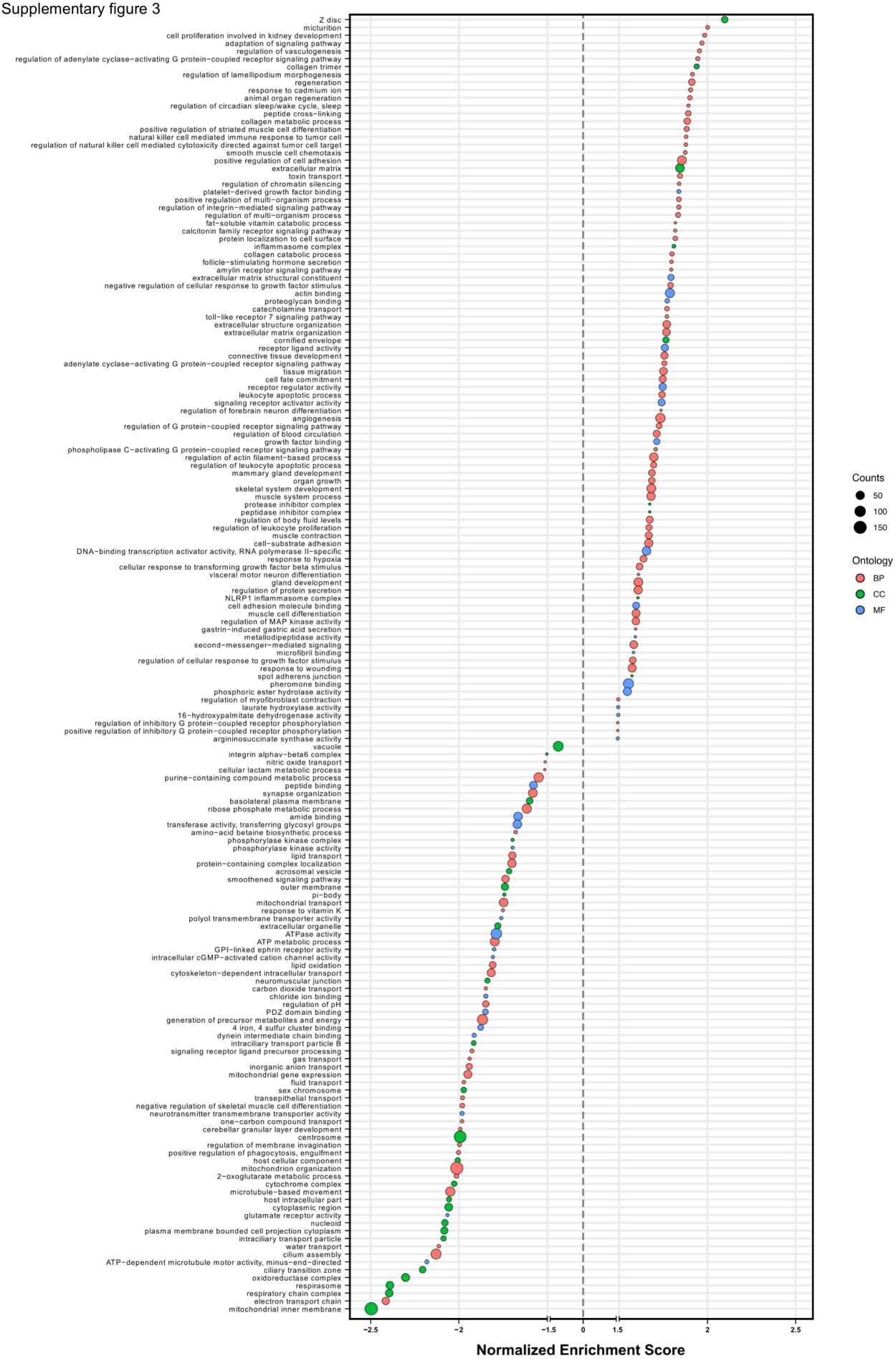

Supplemental Figure 3. Normalized enrichment scores from gene set enrichment analysis of microarray data. (A) Dot plot of normalized enrichment scores for terms in upregulated and downregulated gene sets generated from gene set enrichment analysis of microarray data. Enriched gene ontology terms (Biological process (BP), Cell component (CC) and Molecular Function (MF)) are represented by dot colour and the relative abundance of genes (counts)/ term is indicated by dot size.

Supplementary figure 4

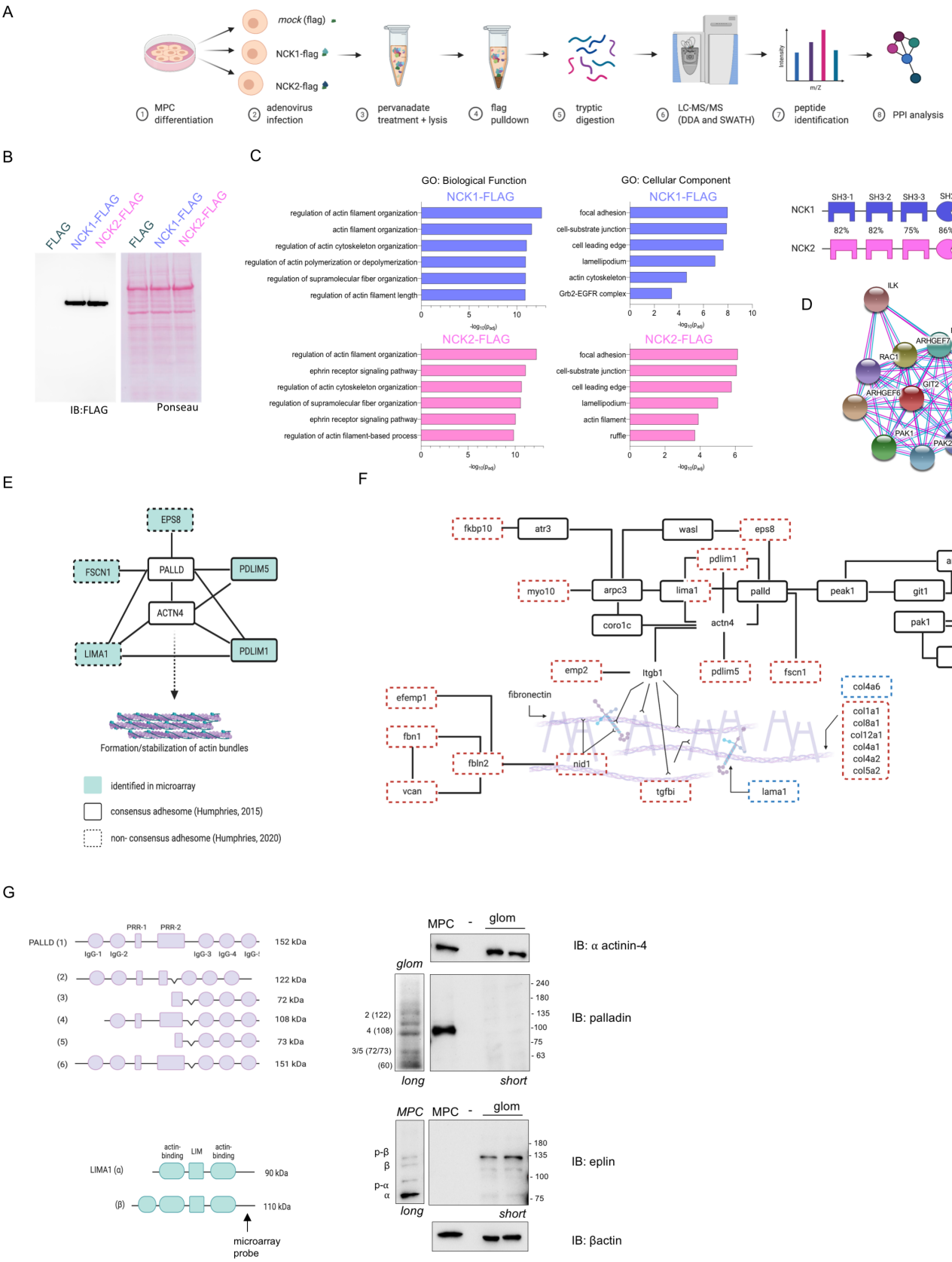

Supplemental Figure 4. Multi-faceted contributions of Nck1 and Nck2 to α actinin-4 and ß1 integrin-related cell adhesion. (A) Experimental workflow for affinity purified mass spectrometry (AP-MS)-based identification of NCK1 and NCK2 protein interactors in mouse podocyte cells (MPCs). FLAG-NCK1, FLAG-NCK2 or FLAG (control) 'baits' were delivered using adenovirus in differentiated WT podocytes and subsequently affinity purified alongside interacting 'prey' proteins from cell lysates (B) Ponceau staining and flag immunoblot (IB) of samples used for AP-MS. (C) Gene ontology (GO) analysis of biological function and cellular componentry of preys captured by NCK1 or NCK2 and identified by AP-MS. NCK1 and NCK2 binding domain homology is high, as is the similarity of the enrichment terms identified. (D) String enrichment of ßPix, GIT, PAK and Nck. (E) Relationship between α actinin-4 binding partners (as identified by string) that were also identified as upregulated genes in Nck1 and 2 double knockout (dKO) cells by microarray. (F) Established interactions (identified by string) between NCK1 and NCK2 interactors identified by AP-MS and genes >2-fold mis-regulated by microarray that are relevant to α actinin-4 and ß1 integrin-related cell adhesion. Red boxes indicate upregulated genes while blue boxes represent downregulated genes. (G) Isoform structure and protein expression profiles of eplin and palladin in MPCs and mouse glomerular samples. Palladin expression was restricted to a ~108 kDa isoform in wildtype podocyte cells. Conversely, several palladin isoforms could be detected in mouse glomerular samples, albeit in low abundance compared to cultured cells. On the contrary, eplin was highly expressed in glomerular samples and a band likely corresponding to the ß isoform was enriched, while expression of a band corresponding to the presumed α isoform was predominant in cultured podocytes. Interestingly, in cells exposed to shear stress, eplin's ß isoform predominates and functions in actin bundle stabilization[84]. Conversely, eplin's α isoform is more widely expressed and contributes to actin dynamics through its inhibition of Arp2/3 actin branching downstream of WASp/WAVE. Doublets of each eplin isoform were observed, the possible result of phosphorylation events, which increase eplin's affinity for actin[85].

Supplementary figure 5

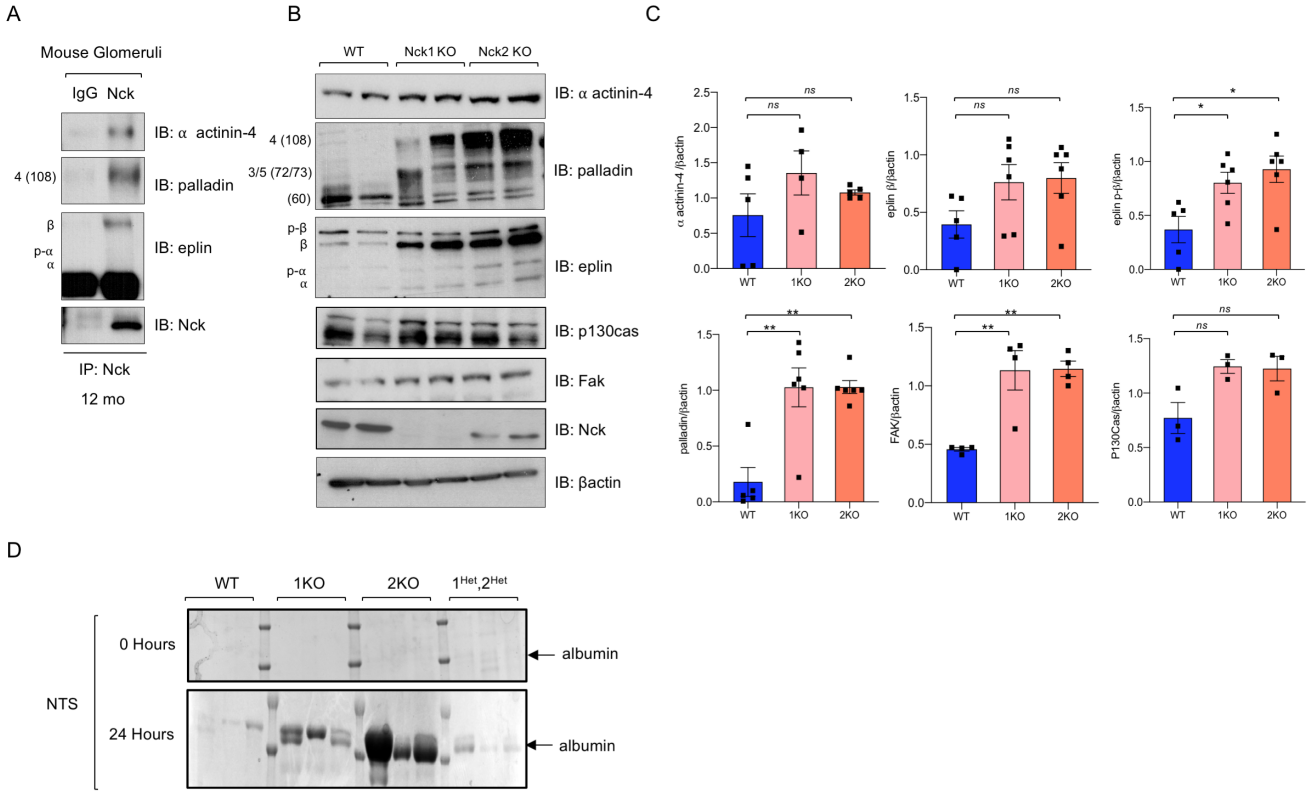

Supplemental Figure 5. Loss of Nck1 or Nck2 (but not Nck1/2 haploinsufficiency) results in biochemical abnormalities and susceptibility to disease. (A) Co-immunoprecipitation (IP) of Nck with α actinin-4, palladin and eplin from glomerular lysates of wildtype (WT) mice. (B) Immunoblotting (IB) and densitometric quantification (C) of glomerular lysates from wildtype (WT), Nck1 knockout (Nck1KO) and Nck2KO mice at 8 weeks of age. (C) Coomassie urine gel of WT, Nck1KO, Nck2KO, and Nck1-/+, Nck2-/+ (double heterozygous) at the peak timepoint (24 hours) of nephrotoxic serum (NTS) induced-disease.

Supplemental References

83. Lussier G, Larose L: A casein kinase I activity is constitutively associated with Nck. *J. Biol. Chem.* 272: 2688–2694, 1997

84. Maul RS, Song Y, Amann KJ, Gerbin SC, Pollard TD, Chang DD: EPLIN regulates actin dynamics by cross-linking and stabilizing filaments. *J. Cell Biol.* 160: 399–407, 2003

85. Han M-Y, Kosako H, Watanabe T, Hattori S: Extracellular signal-regulated kinase/mitogen-activated protein kinase regulates actin organization and cell motility by phosphorylating the actin cross-linking protein EPLIN. *Mol. Cell. Biol.* 27: 8190–8204, 2007